Discrete element modelling of agglomerate impact using autoadhesive elastic-plastic particles

Liu, Lianfeng; Thornton, Colin; Shaw, Stephen James; Tadjouddine, Emmanuel M.

DOI:
10.1016/j.powtec.2016.04.009

Accepted Manuscript

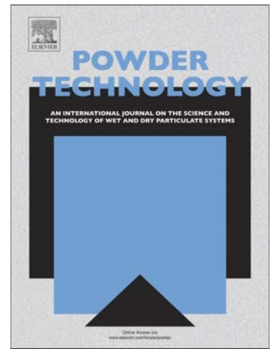

Discrete element modelling of agglomerate impact using autoadhesive elastic-plastic particles

Lianfeng Liu, Colin Thornton, Stephen James Shaw, Emmanuel M. Tadjouddine

PII: S0032-5910(16)30168-1
DOI: doi: 10.1016/j.powtec.2016.04.009
Reference: PTEC 11596

To appear in: *Powder Technology*

Received date: 9 October 2015
Revised date: 2 February 2016
Accepted date: 7 April 2016

Discrete Element Modelling of agglomerate impact using autoadhesive elastic-plastic particles

Lianfeng Liu [1*], Colin Thornton [2], Stephen James Shaw [1], Emmanuel M. Tadjouddine [1]

1. Department of Mathematical Sciences, Xi'an Jiaotong-Liverpool University
111 Ren Ai Road, Dushu Lake Higher Education Town, Suzhou, JiangSu, 215123, China

2. School of Chemical Engineering, The University of Birmingham,
Edgbaston, Birmingham, B15 2TT, United Kingdom

Abstract. In this study, the impact of agglomerates composed of autoadhesive, elastic-plastic primary particles are simulated using the Discrete Element Method. Results obtained are compared to the impact breakage of an agglomerate of autoadhesive elastic particles. It is found that, for the same impact velocity, the elastic agglomerate fractures but the elastic-plastic agglomerate disintegrates adjacent to the impact site. For the elastic-plastic agglomerate, the impact damage increases with increase in material yield stress. It is also found that the particle size distribution of the debris is more accurately defined by a logarithmic function rather than the power law function commonly obtained for impacts of agglomerates composed of elastic particles.

Keywords: Agglomerates; Discrete Element Method; impact breakage;

[*]Corresponding author, E-mail address: David.Liu@xjtlu.edu.cn

1. Introduction

Particulate materials are frequently in the form of powders which are themselves agglomerations of much smaller sized primary particles. A common problem inherent in the handling of powders is the degradation resulting from attrition and/or fragmentation of agglomerates as they collide with each other and with the process equipment. Impact breakage has been studied experimentally for many years [1-9]. However, information from such experiments is normally restricted to post-impact examinations of the fragments and debris produced due to the short duration of an impact event. Numerical simulations of agglomerate impact fracture can overcome these restrictions and, therefore, have been extensively used to simulate impacts of agglomerates. Notable research findings have been made by Thornton and co-workers [10-18] by using the discrete element method [19, 20] based upon contact mechanics [21]. Thornton et al. [10] reported results of 2D simulations of agglomerate impact and demonstrated that the energy required to break the interparticle bonds was orders of magnitude less than the initial work input. Three-dimensional simulations of impacts of a crystalline agglomerate were presented by Kafui and Thornton [14]. It was shown that the proportion of bonds broken during an impact was proportional to $\ln(V/V_0)$ where V is the impact velocity and V_0 is the threshold velocity below which no significant damage occurred. The threshold velocity V_0 was found to scale with $\Gamma^{3/2}$ were Γ is the interface energy between contacting particles. From 3D simulations of the normal impact of a polydisperse (irregular array) spherical agglomerate [11, 12] it was shown that higher impact velocities lead to higher platen forces, local contact damage, number of broken bonds and amount of debris produced. It was demonstrated that rebound, fracture or shattering could occur depending on the magnitude of the impact velocity and the strength of the interparticle bonds.

Mishra and Thornton [15] demonstrated that dense agglomerates always fracture (above a critical impact velocity) but loose agglomerates always disintegrate. They showed that either fracture or disintegration may occur for agglomerates with an intermediate packing density and that the mode of breakage can change from disintegration to fracture by either increasing the interparticle contact density or by changing the location on the agglomerate surface that is used as the impact site. From simulations of the normal impact of a cuboidal agglomerate with a planar target wall, Thornton and Liu [16] showed that fracture occurs as a result of the heterogeneous distribution of the strong force transmission into the agglomerate that, due to the consequent heterogeneous distribution of particle decelerations, creates a heterogeneous velocity field. It was shown that this produces shear weakening along strong velocity discontinuities that subsequently become the potential fracture planes. If, for whatever reason, strong forces are unable to propagate into the agglomerate then fracture does not occur and the breakage mechanism is one of progressive disintegration.

Given the fact that in the processing industries not all granulation processes produce spherical or near-spherical agglomerates, simulations of the impact breakage of cuboidal and cylindrical agglomerates were presented by Liu et al. [18]. It was found from the simulations that cuboidal edge, cylindrical rim and cuboidal corner impacts generate less damage to the agglomerates. Detailed examinations of the evolutions of damage ratio, wall force and mass distribution of fines produced after impact indicated that the size of the initial contact area, the rate of change of the contact area, together with the local microstructure at the impact site play important roles in agglomerate breakage behaviour. Internal damage to the agglomerate is closely related to the particle deceleration adjacent to the impact site.

On the other hand, intensive research on agglomerate impact has also been carried out by many other researchers to examine various possible influence factors on agglomerate impact. These include particle size and bond strength [22, 23], impact angle [24, 25], interface energy [26] and energy dissipation [27]. There is perhaps one factor that hasn't been fully examined so far, i.e., particle plastic deformation at contacts during an agglomerate impact. We believe that this issue needs to be addressed in granular material impact because high stress concentration at particle contacts during particle collisions can occur, and the resultant inter-particle energy loss could directly affect the mechanisms of attrition and breakage of the agglomerate. Hence, this study focusses specifically on this problem and preliminary research results obtained are presented in the following sections.

2 Numerical methodology and agglomerate preparation procedures

2.1 Granular dynamics

The granular dynamics model used in this study originated as the distinct element method (DEM), [19]which was extended to 3D applications by the development of the program TRUBAL, Cundall [20].

In DEM simulations, the particle interactions are modelled as a dynamic process, the evolution of which is advanced using an explicit finite difference scheme to obtain the incremental contact forces and then the incremental displacements of the particles, both linear and rotational. Each cycle of calculations that takes the system from time t to time t + Δt involves the application of incremental force–displacement interaction laws at each contact, resulting in new interparticle forces that are resolved to obtain new out-of-balance forces and moments for each particle. Numerical integration of Newton's second law of motion yields the new linear and rotational velocities for each particle. A second integration yields the incremental particle displacements and, using the new particle velocities and positions, the calculation cycle is repeated in the next time step. The time step Δt used is a fraction of the critical time step determined from the Rayleigh wave speed for the solid particles. For complete details of the granular dynamics methodology the reader is referred to Thornton [21].

The version of the DEM code adapted to simulate agglomerates (and renamed GRANULE) is capable of modelling elastic, frictional, adhesive or non-adhesive spherical particles with or without plastic yield at the interparticle contacts. For the agglomerate impact simulations reported below we have adopted the adhesive, elastic contact force model of Thornton and Yin [28] and the adhesive, elastic-plastic contact force model of Thornton and Ning [29]. Full theoretical details of these models can be found in [28], [29] and [21].

2.2 Preparation of an agglomerate

We have chosen to prepare a cuboidal agglomerate of particles in this research because it bears some 'attractive' characteristics such as having corners and edges which potentially allow us to be flexible to create an impact orientation which would likely exhibit structural changes that are sensitive to plastic deformation during an impact. In addition, for the chosen orientation, the motion is essentially planar and therefore cracks are easily visualised.

The agglomerate consisted of 10,000 primary particles (spheres) with an average diameter of 20 μm and particle size distribution as shown in Fig. 1. For the agglomerate the material properties of the primary particles were specified as: Young's modulus E = 70 GPa, Poisson's ratio $\nu = 0.3$, density $\rho = 2650$ kg/m^3 and interparticle friction coefficient $\mu = 0.35$. The same properties were specified for the stationary planar wall against which the agglomerate was to be impacted.

The procedures used to prepare the agglomerate were as follows. The primary particles were randomly generated in a specified cuboidal volume sufficiently large that there were no interparticle contacts. With interparticle friction set at a low value and using a time step of Δt =

8.52 ns per cycle, a centripetal gravity field was then increased to g = 10 m/s^2 and cycling continued. During this stage the decrease in porosity and increase in the number of contacts was monitored. After approximately 1 million cycles further changes in these two parameters were insignificant, at which point the time step was reduced by a factor of 10 and the interparticle friction coefficient was increased in steps of 0.02 to a final value of 0.35 with 10K cycles being carried out for each step increase. At the same time, surface energy was introduced at the interparticle contacts. The final value of interface energy $\Gamma = 2\gamma = 1.0$ J/m^2 was obtained by step increases in the surface energy of the individual particles of $\Delta\gamma = 0.01$ J/m^2 initially and then $\Delta\gamma = 0.05$ J/m^2. The centripetal gravity was then reduced in small steps to zero. The final, as prepared, porosity of the cuboidal agglomerate was 0.42, with a corresponding bulk density of 1153.10 kg/m^3. At the end of the preparation stage the coordination number of the cuboidal agglomerate was 3.52, corresponding to 14,993 contacts in the agglomerate. Fig. 2 shows views of the cuboidal agglomerate as prepared by the procedures described above. The dimensions of the agglomerate were 0.497mm × 0.445 mm × 0.447 mm. Details of the agglomerate properties can be found in Table 1.

3 Elastic agglomerate impact

For comparison, we first carried out impact simulations of an agglomerate composed of elastic particles onto a target wall. Plastic deformation of the particles was not allowed by defining the material yield strength as 7.0E30 Pa. Impact simulations begin by setting a velocity to all the agglomerate particles in the vertical direction. The cuboidal agglomerate was orientated in order to have one of it edges impacted onto the wall underneath. Figure 3 shows the results of an elastic agglomerate impacting the target wall at two different velocities. As seen in the figure, for an impact speed of 1.0 m/s, the agglomerate does not fracture; however, for a speed of 2 m/s, the agglomerate fractures.

The proportion of bonds broken during an impact is defined as the damage ratio D and written as:

$$D = {}^{N_b}\!\big/_{N_0} \qquad (1)$$

where N_b is the number of broken contacts, and N_0 is the total number of initial contacts within the agglomerate.

It is useful to clarify the terminology that will be adopted to describe the observed breakage phenomena following Thornton and Liu [16]. The term ‘‘fracture’’ is reserved for breakage patterns in which clear fracture planes (cracks) are visible. This mode produces two or more large daughter fragments and is normally accompanied by some fines production adjacent to the impact site. An alternative mode of breakage is one in which there is no evidence from the simulation data of any attempted fracture and the end products consist of one cluster centred in the upper part of the agglomerate with the remainder of the agglomerate reduced to small clusters of primary particles and singlets. This type of breakage is termed ‘‘disintegration’’. If the impact velocity is sufficiently high that disintegration extends throughout the agglomerate and there is no ‘‘large’’ surviving cluster then this mode is referred to as ‘‘total disintegration’’. If total disintegration occurs the agglomerate simply collapses into a heap on the target wall.

Observations of agglomerate impact reveal that the impact process causing internal damage to the agglomerate can be divided into two phases (Fig. 3). First, during the initial stage of the impact, an observable ‘damage zone’ (Fig. 3b) is formed at the contact area between the agglomerate and the target wall as forces are transmitted into the agglomerate from the wall. The microstructure of the constituent particles near the wall contact area experience "irreversible" deformation (Fig. 3b), during which time, sliding occurs between the particles, the internal restructuring takes place and micro-cracks are generated, distributed randomly along the compression direction.

Typical time evolutions of the force generated at the agglomerate-wall interface, the kinetic energy of the system of primary particles composing the agglomerate and the proportion of initial interparticle bonds broken during the impact are shown in Fig. 4 (the impact velocity of the particle system is 2 m / s, the interface energy between the particles is 1.0 J/m^2).

As shown in Fig. 4, the wall force increases rapidly and reaches a relatively stable peak region (Fig. 4a) and the damage ratio increases rapidly and the total kinetic energy of the system continuously decreases (as shown in Fig. 4b) . Thus, this process can be considered as a "loading" process.

The second stage is a selective bond breaking process in that some of the micro-cracks continue to develop along the compression direction from the "damage zone" and spread to form cracks or fractures (shown in Fig. 3b). The wall force decreases to a small value (Fig. 4a) comparable with the self-weight of the agglomerate. This process can be regarded as the "unloading" period of the impact. During this process, the damage ratio continues to increase at a significantly reduced rate (Fig. 4b), the total kinetic energy reduces to its minimum value indicating that the degree of damage to the agglomerate due to particle bond rupture has completed.

In the above two impact tests on the elastic agglomerate, it is clearly seen that agglomerate fracture occurred for a velocity V = 2.0 m/s. Therefore, we take this case as a reference to make comparisons with the following impact tests on elastic-plastic agglomerates.

4 Elastic-plastic agglomerate impact

Initially a number of impacts were simulated using a range of values for the limiting contact pressure p_y from 10 GPa down to 1.5 GPa. It was found that, for $p_y \leq 3$ GPa, particles in the damage zone of the agglomerate start to yield. Therefore, in the following study, we first set p_y = 2.3 GPa as a typical case to examine the mechanism of impact damage for elastic-plastic agglomerates.

In simulations of impact of the agglomerate composed of elastic-plastic spheres, the agglomerate used is exactly the same as the agglomerate composed of elastic particles except for the predefined limiting contact pressure, i.e. p_y = 2.3 GPa, V = 2 m/s. Figure 5 illustrates the agglomerate after the impact (the snapshots are taken at the same moment as for the elastic impact, i.e. at time = 100 μs) . Surprisingly, unlike the elastic agglomerate impact (Fig. 3b) when the agglomerate was fractured, the elastic-plastic agglomerate did not fracture completely but largely exhibited disintegration. Figure 5b clearly show the connectivity of particle bonds, indicating that the agglomerate remained almost intact although there is a potential inclined fracture plane, a lot of broken bonds near the impact area (broken bonds are not displayed in Fig. 5b), and a 'damage zone' (Fig. 5c) near the wall. From these observations, it follows that, under the same conditions, the only reason for the elastic-plastic agglomerate not fracturing completely is that certain particles have undergone plastic deformation, which results in extra dissipation of kinetic energy.

Figure 6 compares the evolution of impact parameters. A comparison of the wall forces generated during the impacts is provided in Fig. 6a. It can be seen that, for the elastic agglomerate, a maximum wall force of 5.37 mN occurred after 13 μs. For the elastic-plastic agglomerate, a maximum wall force of 6.87 mN occurred after 20 μs. Both agglomerates exhibited significant fluctuations in the wall force evolution but the amplitudes of the fluctuations were smaller for the elastic-plastic agglomerate. It is also noted that there is a fast unloading of the wall force after 33 μs. Figure 6b shows the evolution of the damage ratio for the two agglomerates. The results show that the internal damage of the elastic-plastic agglomerate is initially smaller but, at 16 μs, when the wall force first reaches the maximum value, there is a sudden increase in the damage ratio until 20 μs, when the wall force again reaches the maximum value. Thereafter, the internal damage of the elastic-plastic agglomerate remains higher than that of the elastic agglomerate until, after 51 μs, the two damage ratios are very similar. The evolution of the kinetic energy (normalised by the initial kinetic energy) is shown in Fig. 6c. The figure shows that the decay in kinetic energy is faster for the elastic-plastic agglomerate.

Although the elastic-plastic agglomerate did not fracture completely, the internal damage caused was smaller at first then larger than that for the elastic agglomerate impact. Interestingly, the elastic-plastic agglomerate produced a higher maximum wall force (6.87 mN) than the elastic agglomerate (5.37 mN). This phenomenon implies that, due to plastic deformation of a portion of the particles in the agglomerate, the transmission of the shockwave (or forces) was retarded and its speed tended to be decreased. A larger wall force was generated in the elastic-plastic agglomerate impact because the shockwave could not penetrate to release the kinetic energy faster.

5 Effects of impact velocity and limiting contact pressure

In three-dimensional agglomerate impact simulations, the effects of velocity is one of the factors which have been examined most frequently. The general conclusion is that agglomerate damage becomes more sever with increased impact velocity. Research in this area can be found in [13] [11] [12] and [14]. However, these studies generally do not consider plastic deformation of the primary particles. Kafui et al [13] proposed that the damage ratio is a function of the Weber number which is

$$W_e = \rho V^2 d / \Gamma \tag{2}$$

where ρ is the particle density, V is the impact velocity, d is the average particle diameter, and Γ is the interface energy. However, the above theory was found not to be applicable to the case when the velocity is sufficiently small. Thornton et al. [10] introduced a threshold velocity V_0, below which the agglomerate has no obvious damage after impact and suggested an amendment of the Weber number, which is

$$W_e^{'} = \rho (V - V_0)^2 d / \Gamma \tag{3}$$

The relationships can be used for the analysis of agglomerate damage ratio after impact. Similarly, Ghadiri and Papadopoulos [30] presented an attrition propensity parameter η, which has the following relationship

$$\eta \sim \left(\rho V^2 d / \Gamma\right)\left(\sigma_y / E\right) \tag{4}$$

where the first factor in the formula is the Weber number.

In the following study, we examine the effect of impact velocity on the damage ratio under the condition that plastic deformation at particle contacts occurs. Figure 7 shows the evolution of impact parameters. Considering the wall forces, Fig. 7a indicates that, ignoring the strong fluctuations, the evolution of the wall forces during loading is essentially similar for all three cases. As expected, comparing the two elastic-plastic impacts, the smaller impact velocity produced a smaller peak wall force at a shorter elapsed time. In addition, there was no sudden drop in the wall force when, for the elastic-plastic agglomerate, the impact velocity was reduced from 2.0 m/s to 1.5 m/s. The damage ratio reduced significantly when the elastic-plastic agglomerate was impacted at a velocity of 1.5 m/s, which was less than that developed elastic agglomerate, see Fig. 7b. Figure 7c shows that the rate at which the normalized kinetic energy decreased for the elastic-plastic impact was less when the impact velocity was reduced to V = 1.5 m/s.

Finally, impacts of elastic-plastic agglomerates using different values of p_y have been simulated. The results are shown in Fig.8 in terms of the evolution of damage ratio with time. It can be seen that in general the final damage ratio decreased with decrease in p_y. Since the limiting contact pressure p_y is a function of the yield stress σ_y of the primary particles (i.e. $p_y = 2.5\sigma_y$) it can be understood that a smaller yield stress will result in more yielded particles in the agglomerate, which will consume more kinetic energy and, hence, result in less internal damage to the agglomerate. If we plot the relationship between the final damage ratio and the limiting contact pressure, which is shown in Fig. 9, it can be seen that, for the limited data set examined, the results follow the same trend as Eq. (4) suggested by Ghadiri and Papadopoulos [30], which indicates that the attrition propensity parameter η is proportional to σ_y.

6 Fragment size distribution

In experimental studies, the results of impact breakage can be quantified by examining the fragment size distribution resulting from the impact event. Fig. 10 shows, for all the impacts simulated, a double logarithmic plot of cumulative mass fraction undersize against normalised mass in which the mass of each fragment is normalised by the initial agglomerate mass. The size distribution of the fragments produced by the *elastic* agglomerate impact shows two distinct regions with a sudden change of slope that distinguishes the large fragments (residue) from the complement of small fragments (debris). The bilinear form is in agreement with experimental data, Arbiter et al. [2]. From DEM simulations of spherical agglomerate impacts, Kafui and Thornton [14] demonstrated that the exponent for the debris is independent of the impact velocity but the amount of debris increases with increasing impact velocity. However, Fig. 10 illustrates that, for a given impact velocity, the amount of debris produced is also dependent on particle yield stress. The smallest amount of debris is produced for the lowest yield stress and the largest amount occurs for the highest yield stress. It is, however, notable that there is a region on the plot indicating that medium-sized debris was not produced for all the elastic-plastic agglomerate impacts. As stated previously, this was due to the fact that an elastic-plastic agglomerate tended to disintegrate rather than fracture during an impact. For the simulations reported here, with an interface energy Γ = 1.0 J/m^2 and an impact velocity of 2 m/s, there is also a hint from Fig. 10 that the distribution of the debris gradually deviates from the linear trend as the material yield stress becomes smaller, as seen especially for the case of p_y = 1.8 GPa. Trend lines of the fragment distributions of debris produced by elastic-plastic agglomerate impacts are shown in Fig. 11, which indicate that a logarithmic function can better describe the distribution of debris.

7 Conclusions

Discrete element modelling of agglomerate impact has been conducted by adopting a contact mechanics theory for the interactions of elastic-plastic self-adhesive particles. Results have shown that under the same conditions, other than the predefined limiting contact pressure, the elastic-plastic agglomerates tend to disintegrate during impact in contrast to elastic agglomerates which fracture. Due to the presence of plastic deformation and additional kinetic energy loss, the elastic-plastic agglomerates during impact require a longer loading period than elastic agglomerates, but generate larger peak wall forces and greater internal damage. It was also observed that the amplitude of wall force fluctuations during loading was relatively smaller than for the corresponding elastic agglomerate. Finally, this study has examined the effect of varying the limiting contact pressure on the final damage ratio produced. Preliminary results have shown that the damage ratio is linearly proportional to the limiting contact pressure. Since the limiting contact pressure is a function of the material yield stress (e.g. p_y = 2.5 σ_y) this result is in agreement with Ghadiri and Papadopoulos [30] who suggested that their attrition propensity parameter η is proportional to σ_y. It should be noted that energy loss by elastic wave propagation [31,32] has not been considered in this study, as the impact surface is of finite dimensions especially in the normal direction.

In all cases of elastic-plastic agglomerate impact the cumulative probability of the post-impact fragment size distribution of the debris deviated from the usual power law trend. It was further shown that a logarithmic function can better describe the size distribution of the debris. The current simulation results have demonstrated that the amount of debris is sensitive to the limiting contact pressure and elastic-plastic agglomerates tend to disintegrate during an impact rather than fracture.

Acknowledgements

The authors are grateful for the financial support from the Natural Science Foundation of Jiangsu Province of China (Project No. BK20131179).

References

[1] H. Rumpf, The strength of granules and agglomerates, in W.A. Knepper (Ed.), *Agglomeration*, New York, Interscience, 1962, pp. 379-418.

[2] N. Arbiter, C. C. Harris, G. A. Stamboltzis, Single fracture of brittle spheres, *Transactions of the Society of Mining Engineers AIME* 244, 118-133, 1969.

[3] Y. S. Cheong, A. D. Salman, M. J. Hounslow, Effect of impact angle and velocity on the fragment size distribution of glass spheres, *Powder Technology* 138, 189-200, 2003.

[4] A. D. Salman, G. K. Reynolds, M. J. Hounslow, Particle impact brekage in particulate processing, *KONA Particle and Powder* 21, 88-99, 2003.

[5] A. Samimi, M. Ghadiri, G. A. Boerfijn, R. Kohlus, Effect of structural characteristics on impact breakage of agglomerates, *Powder Technology*130, 428-435, 2003.

[6] J. Subero, M. Ghadiri, Breakage patterns of agglomerates, *Powder Technology* 120, 232-243, 2001.

[7] A. Samimi, R. Moreno, M. Ghadiri, Analysis of impact damage of agglomerates: effect of impact angle, *Powder Technology*143-144, 97-109, 2004.

[8] S. Antonyuk, M. Khanal, J. Tomas, S. Heinrich, Morl, Impact breakage of spherical granules: experimental study and DEM simulation, *Chemical Engineering and Processing* 45, 838-856, 2006.

[9] S. Antonyuk, S. Palis, S. Heinrich, Breakage behaviour of agglomerates and crystals by static loading and impact, *Powder Technology* 206, 88-98, 2011.

[10] C. Thornton, K. K. Yin, M. J. Adams, Numerical simulation of the impact fracture and fragmentation of agglomerates, *J. Phys. D: Appl. Phys.* 29, 424-435, 1996.

[11] C. Thornton, M. T. Ciomocos, K. K. Yin, M. J. Adams, Fracture of particulate solids, in *Powders & Grains 97*, Behringer, R.P. & Jenkins, J.T. (Eds.), Balkema, Rotterdam, 1997, pp. 131-134.

[12] C. Thornton, M. T. Ciomocos, M. J. Adams, Numerical simulations of agglomerate impact breakage, *Powder Technology* 105, 74-82, 1999.

[13] K. D. Kafui, C. Thornton, Computer simulated impact of agglomerates, in *Powders & Grains 93*, Thornton, C. (Ed.), Balkema, Rotterdam, 1993, pp. 401-406.

[14] K. D. Kafui, C. Thornton, Numerical simulations of impact breakage of a spherical crystalline agglomerate, *Powder Technology* 109(1-3), 113-132, 2000.

[15] B. K. Mishra, C. Thornton, Impact breakage of particle agglomerates, *International Journal of Mineral Processing* 61(4), 225-239, 2001.

[16] C. Thornton, L. F. Liu, How do agglomerates break?, *Powder Technology* 143-144, 110-116, 2004.

[17] C. Thornton, L. F. Liu, DEM simulations of uniaxial compression and decompression, in *Compaction of Soils, Granulates and Powders*, Kolymbas, D. & Fellin, W. (Eds.), Balkema, Rotterdam, 2000, Pp. 251-261.

[18] L. F. Liu, K. D. Kafui, C. Thornton, Impact breakage of spherical, cuboidal and cylindrical agglomerates, *Powder Technology* 199(2), 189-196, 2010.

[19] P. A. Cundall, O. D. L. Strack , A discrete numerical model for granular assemblies, *Geotechnique* 29, 47-65, 1979.

[20] P. A. Cundall, Computer simulations of dense sphere assemblies, in *Micromechanics of Granular Materials*, Satake, M. & Jenkins, J.T. (Eds.), Elsevier, Amsterdam, 1988, pp. 113-123.

[21] C. Thornton, *Granular Dynamics, Contact Mechanics and Particle System Simulations – a DEM study*, Particle Technology Series 24, Springer, Dordrecht, 2015.

[22] Z. Ning, R. Boerefijn, M. Ghadiri, C. Thornton, Effects of particle size and bond strength on impact breakage of weak agglomerates, in *Powders & Grains 97*, Behringer, R.P. & Jenkins, J.T. (Eds.), Balkema, Rotterdam, 1997, pp. 127-130.

[23] M. J. Metzger, B. J. Glasser, Numerical investigation of breakage of bonded agglomerates during impact, *Powder Technology* 217, 304-314, 2012.

[24] R. Moreno, J. Ghadiri, S. J. Antony, Effect of the impact angle on the breakage of agglomerates: a numerical study using DEM, *Powder Technology* 130, 132-137, 2003.

[25] Z. B. Tong, R. Y. Yang, A. B. Yu, S. Adi, H. K. Chan, Numerical modelling of the breakage of loose agglomerates of fine particles, *Powder Technology* 196, 213-221, 2009.

[26] R. Moreno-Atanasio, M. Ghadiri, Mechanistic analysis and computer simulation of impact breakage of agglomerates: effect of surface enegy, *Chemical Engineering Science* 61, 2476-2481, 2006.

[27] R. Moreno-Atanasio, Energy dissipation in agglomerates during normal impact, *Powder Technology* 223, 12-18, 2012.

[28] C. Thornton, K. K. Yin, Impact of elastic spheres with and without adhesion, *Powder Technology* 65, 153-166, 1991.

[29] C. Thornton, Z. Ning, A theoretical model for the stick/bounce behaviour of adhesive, elastic-plastic spheres, *Powder Technology* 99, 154-162, 1998.

[30] M. A. Ghadiri, D. G. Papadopoulos, Impact attrition of particulate solids, *International Fine Particle Research Institute Report*, 1995.

[31] J. W. Stronge, Impact mechanics, Cambridge University Press, Cambridge, 2000.

[32] P. Mueller, R. Boettcher, A. Russell, M. Truee, J. Tomas, A novel approach to evaluate the elastic impact of spheres on thin plates, Chem. Eng. Sci. 138,689-697, 2015.

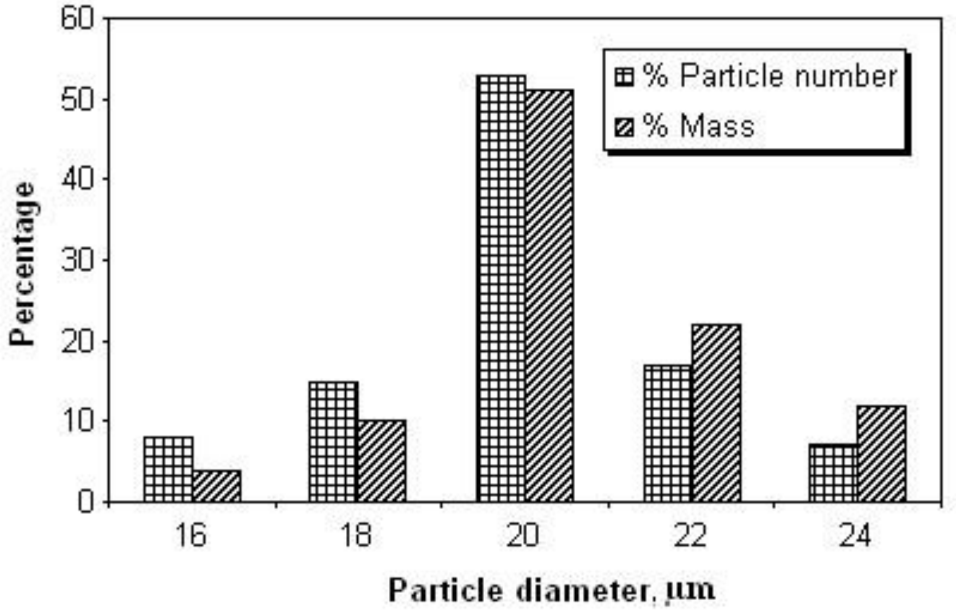

Fig 1 Particle size distribution in the agglomerate

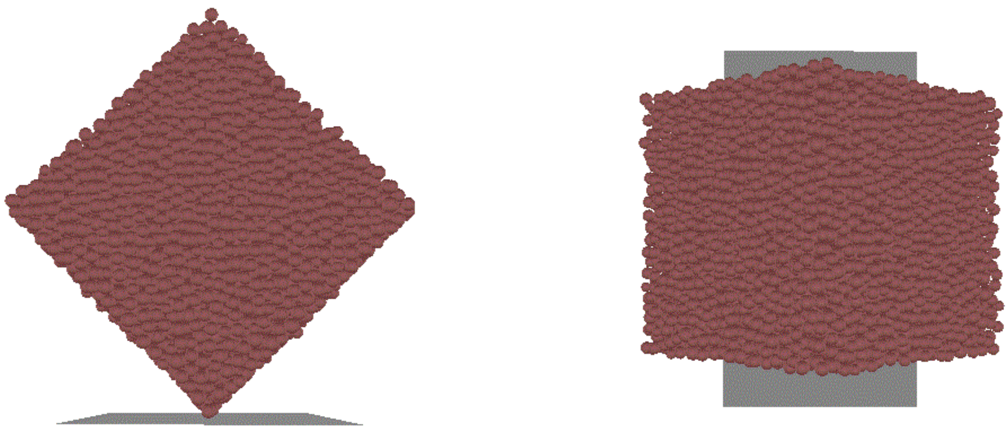

(a) (b)

Fig 2 Cuboidal agglomerate as prepared (a) front view (b) top view

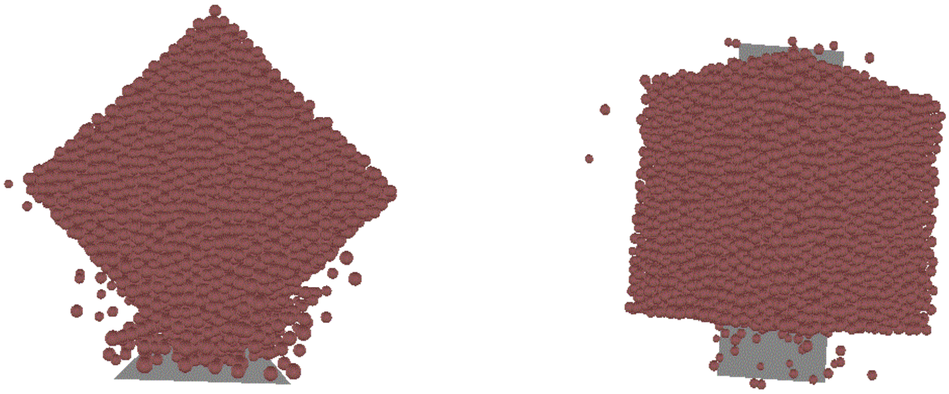

elevation top view

(a) V = 1.0 m/s

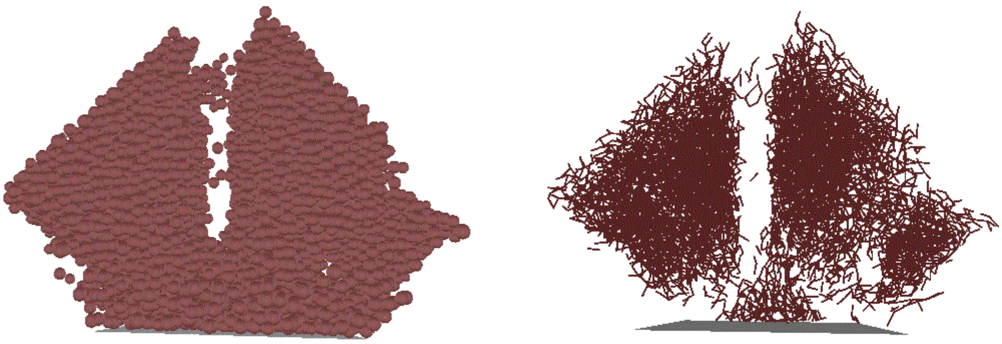

elevation elevation (bond connectivity)

(b) V = 2.0 m/s

Fig 3 Impacts of elastic agglomerates (time = 100 μs)

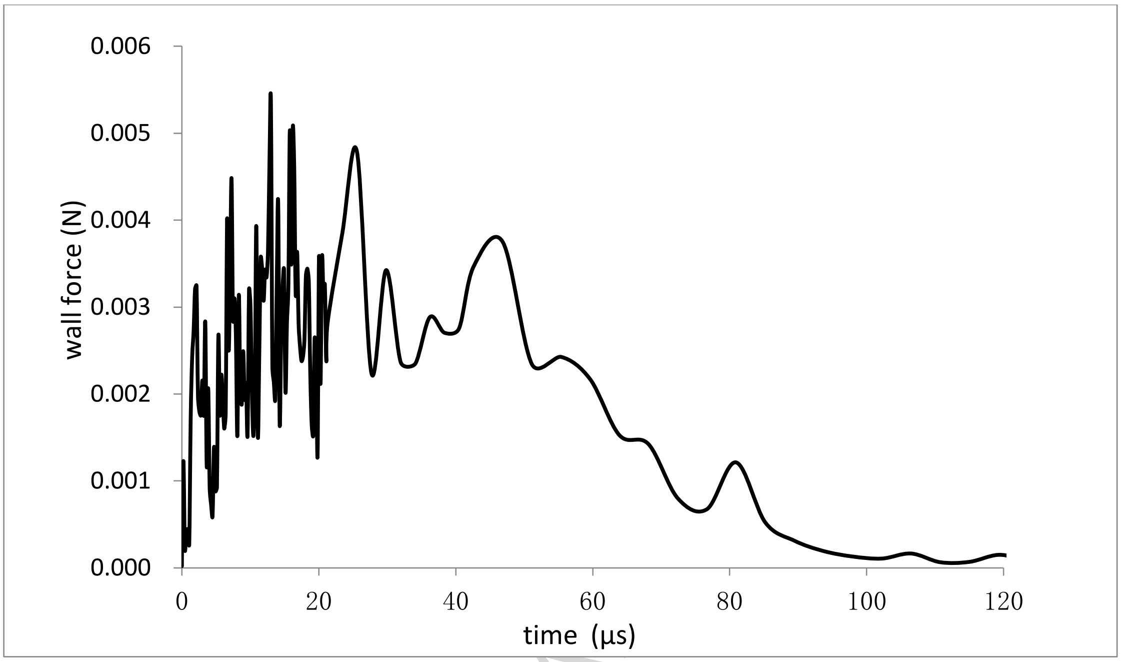

(a) Evolution of wall force with time

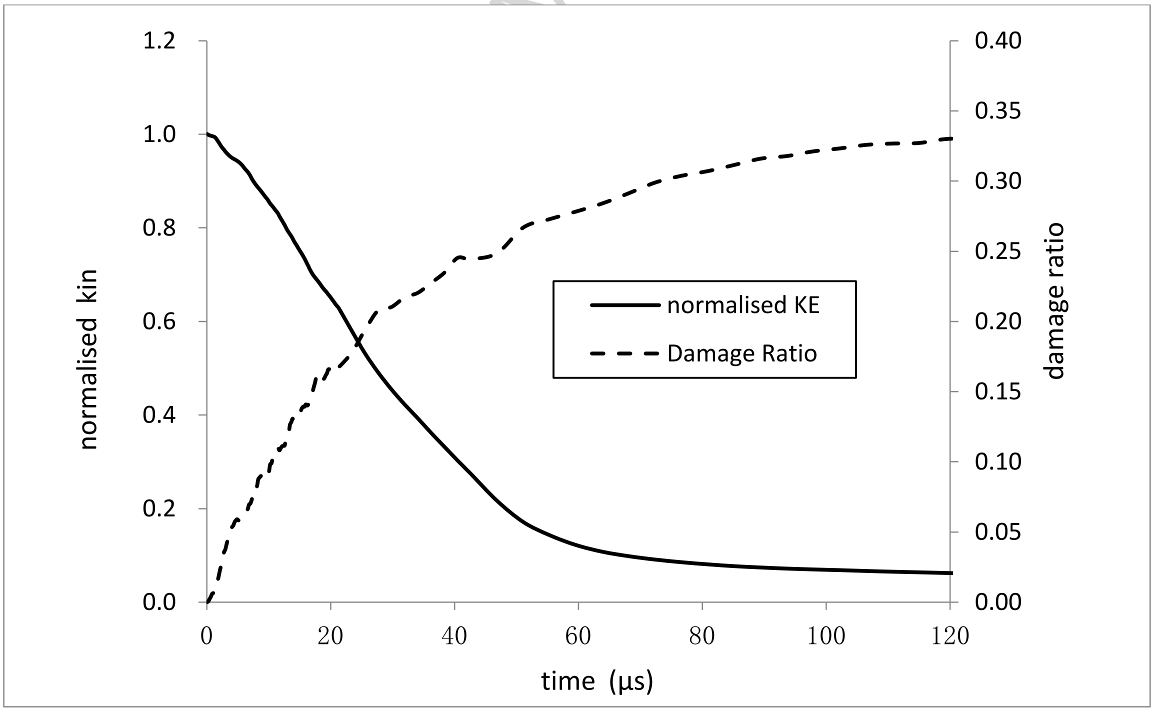

(b) Evolution of damage ratio and normalised kinetic energy with time

Fig 4 Evolution of the impact parameters obtained for an elastic agglomerate (V = 2.0 m/s)

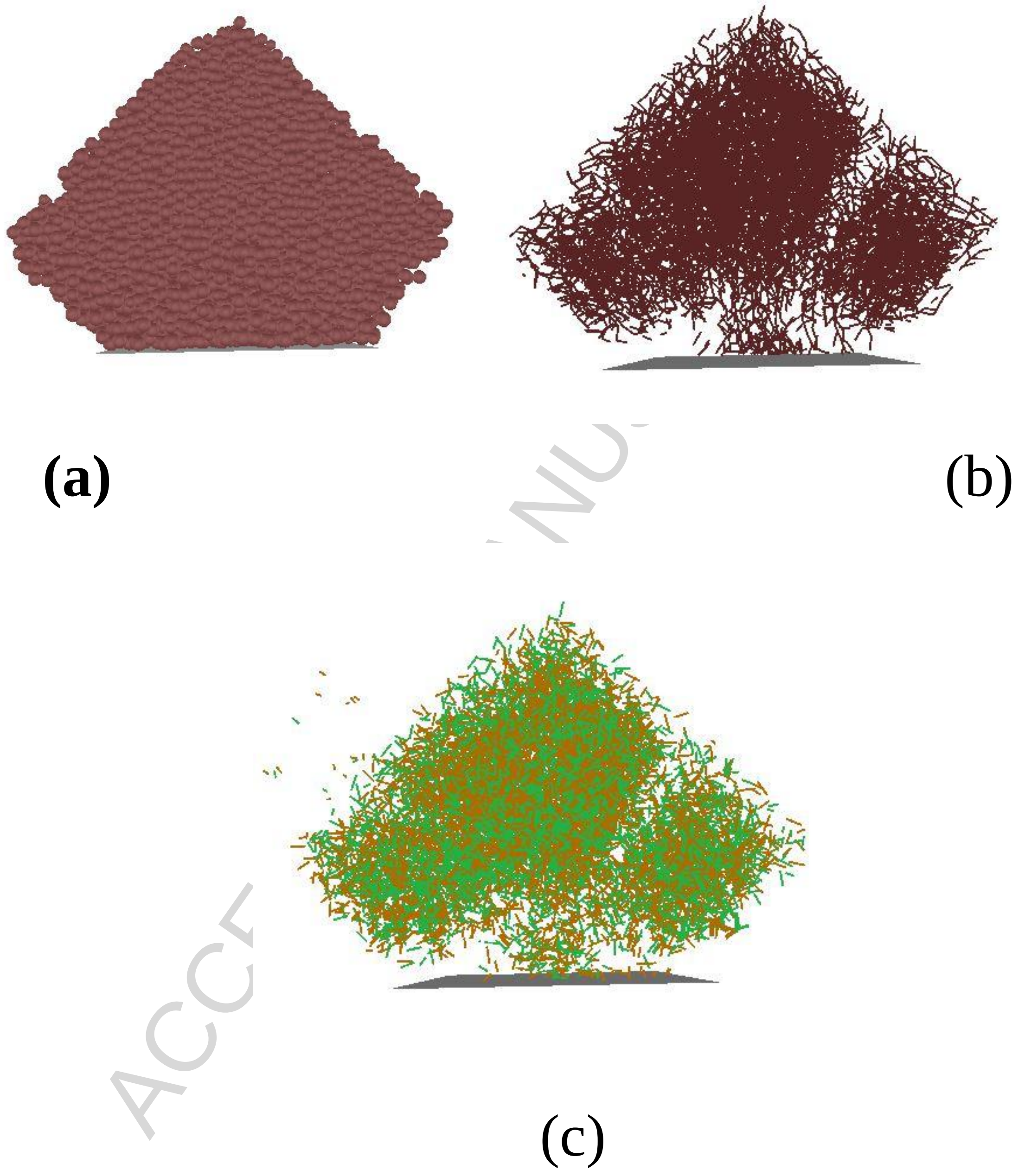

Fig 5 Elastic-plastic agglomerate impact on a target wall (time = 100 µs)

(a) particles (b) connectivity of bonds (c) compressive (brown) and tensile (green) contact forces

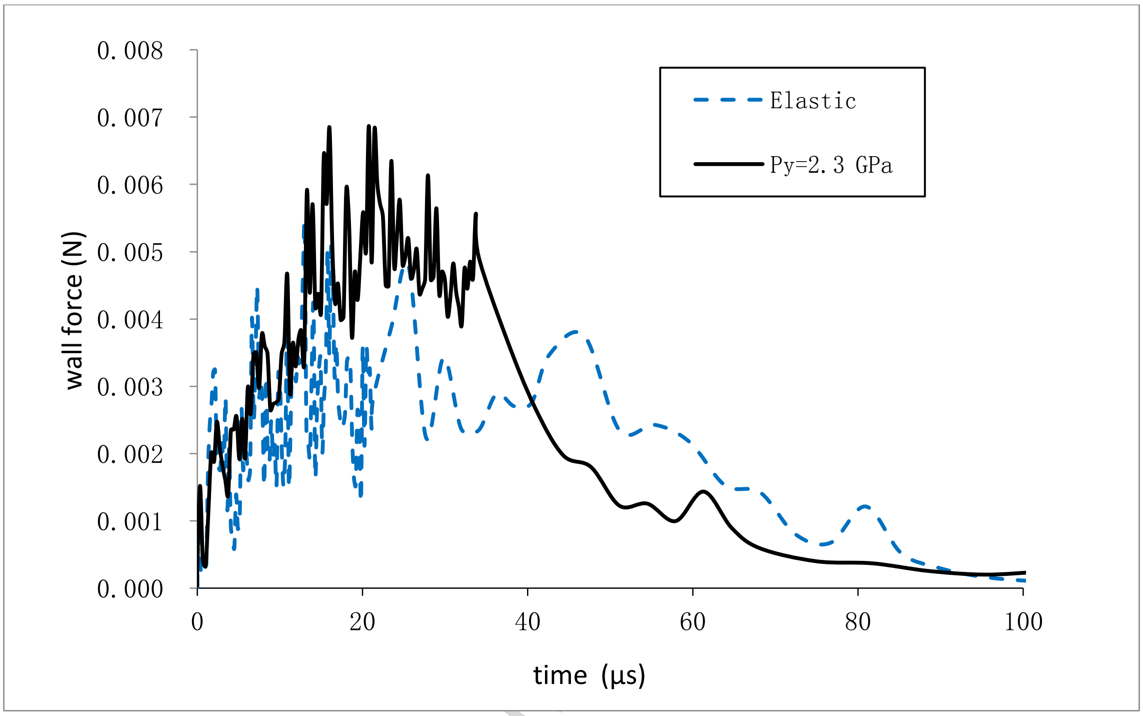

(a) wall force

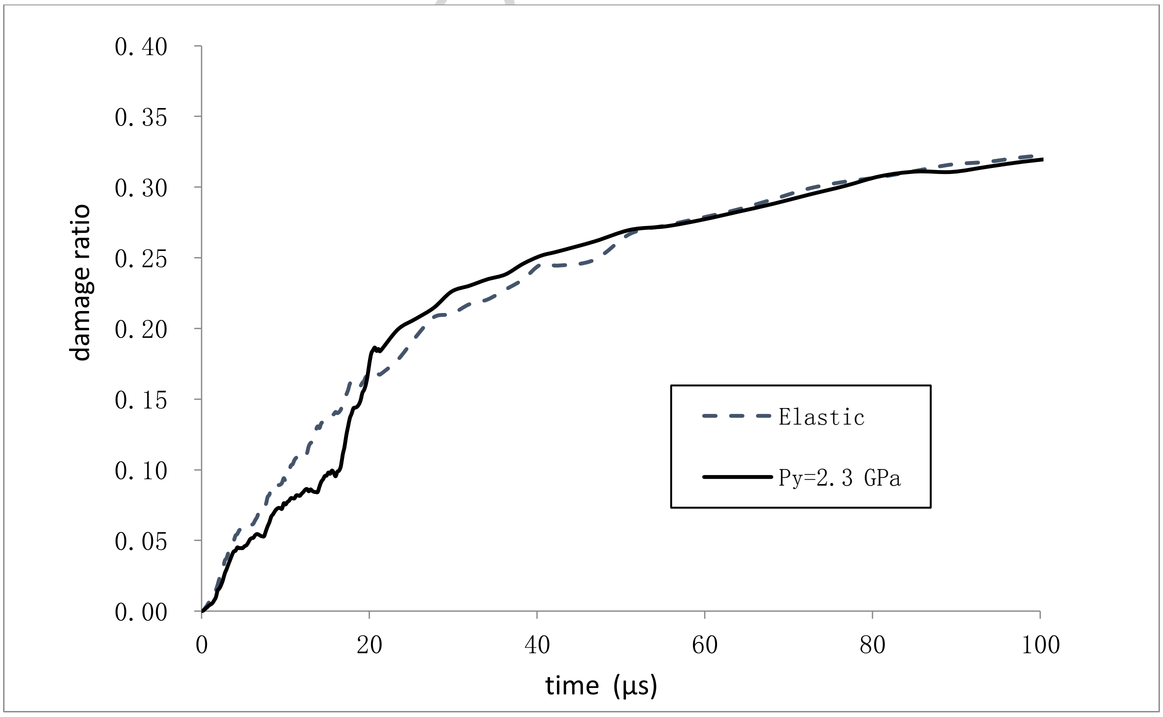

(b) damage ratio

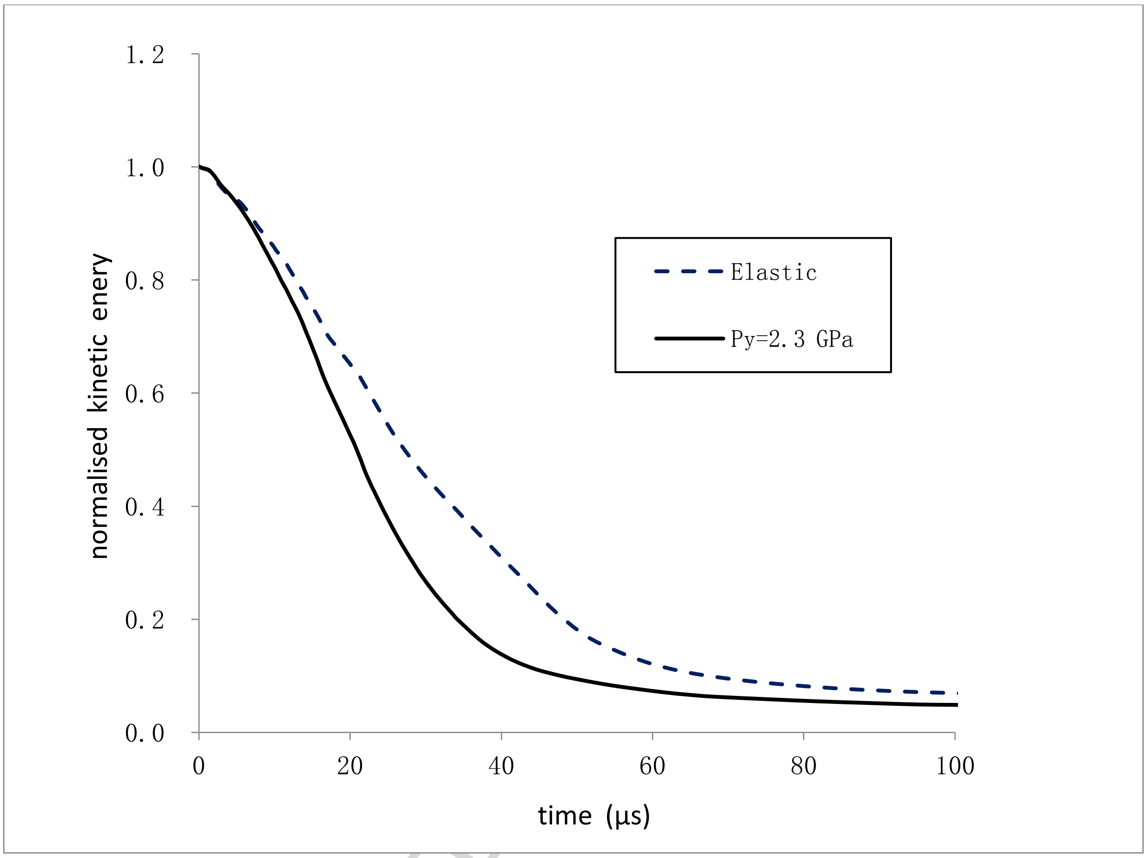

(c) normalised kinetic energy

Fig 6 Comparisions of impact parameters between elastic and elastoplastic agglomerates for V = 2.0 m/s

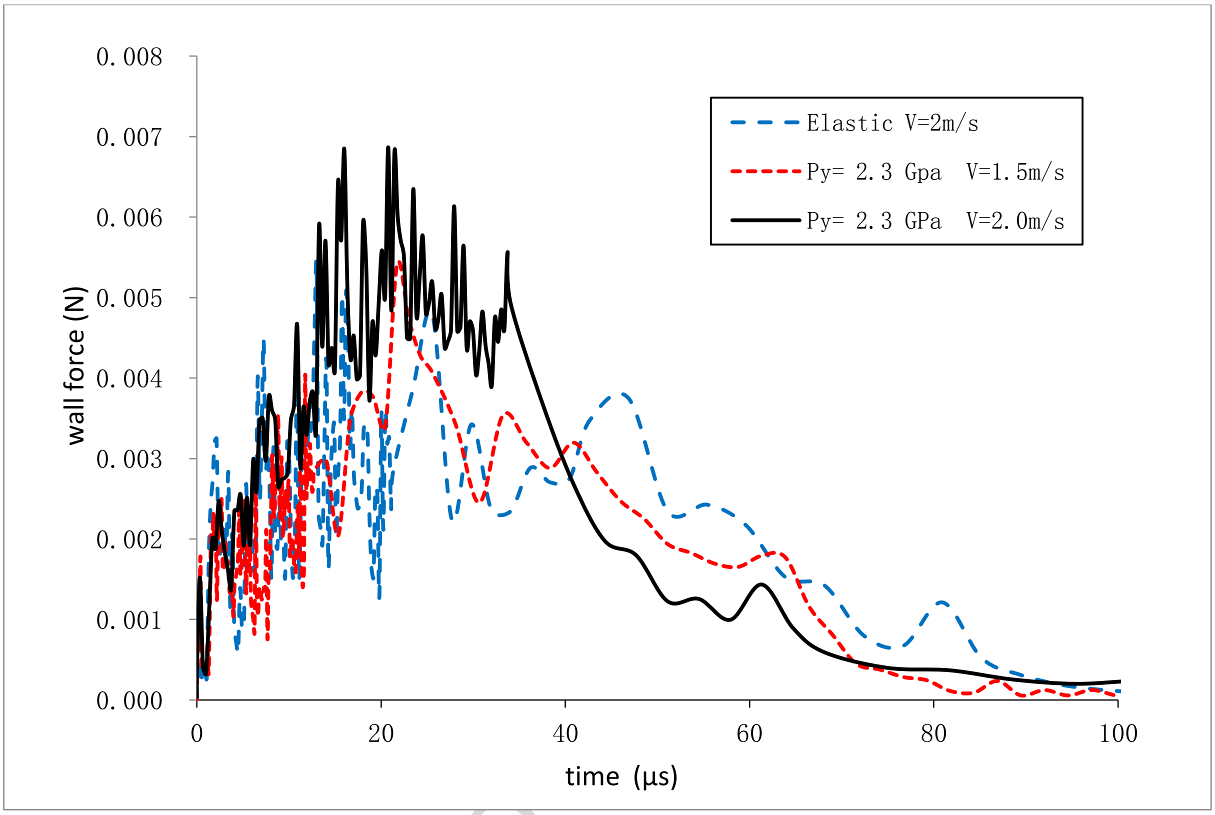

(a) wall force

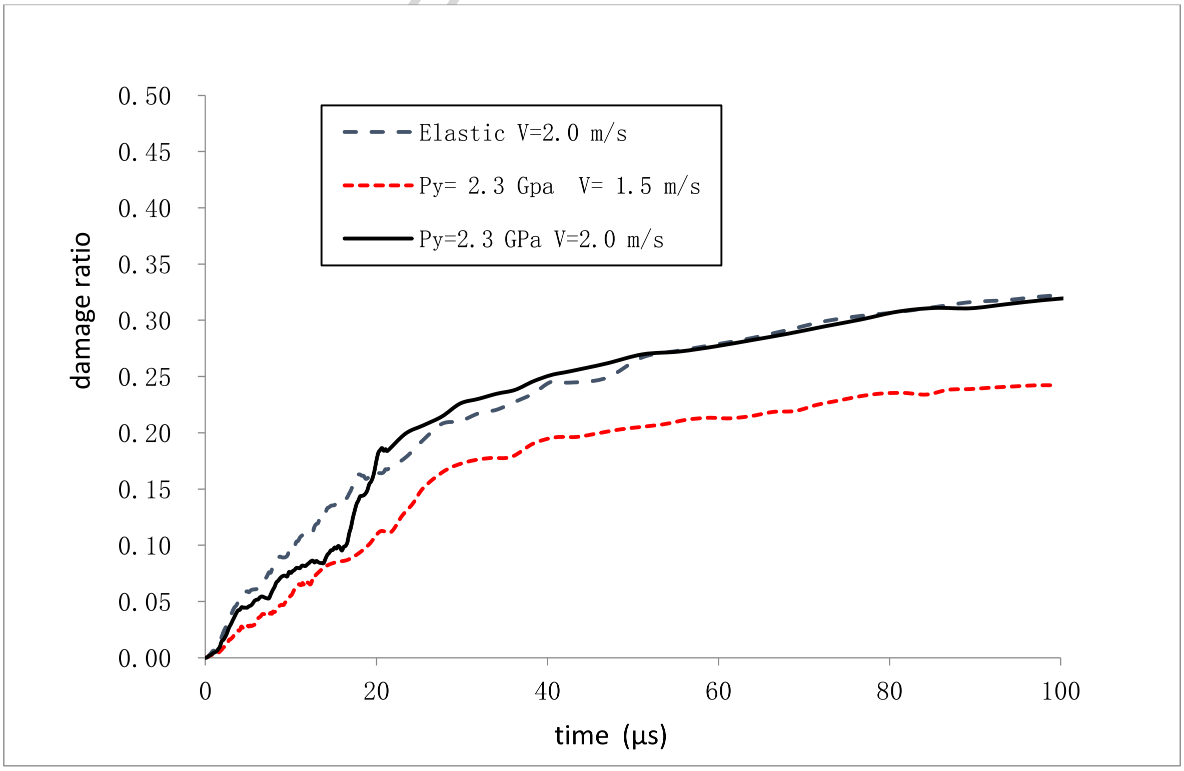

(b) damage ratio

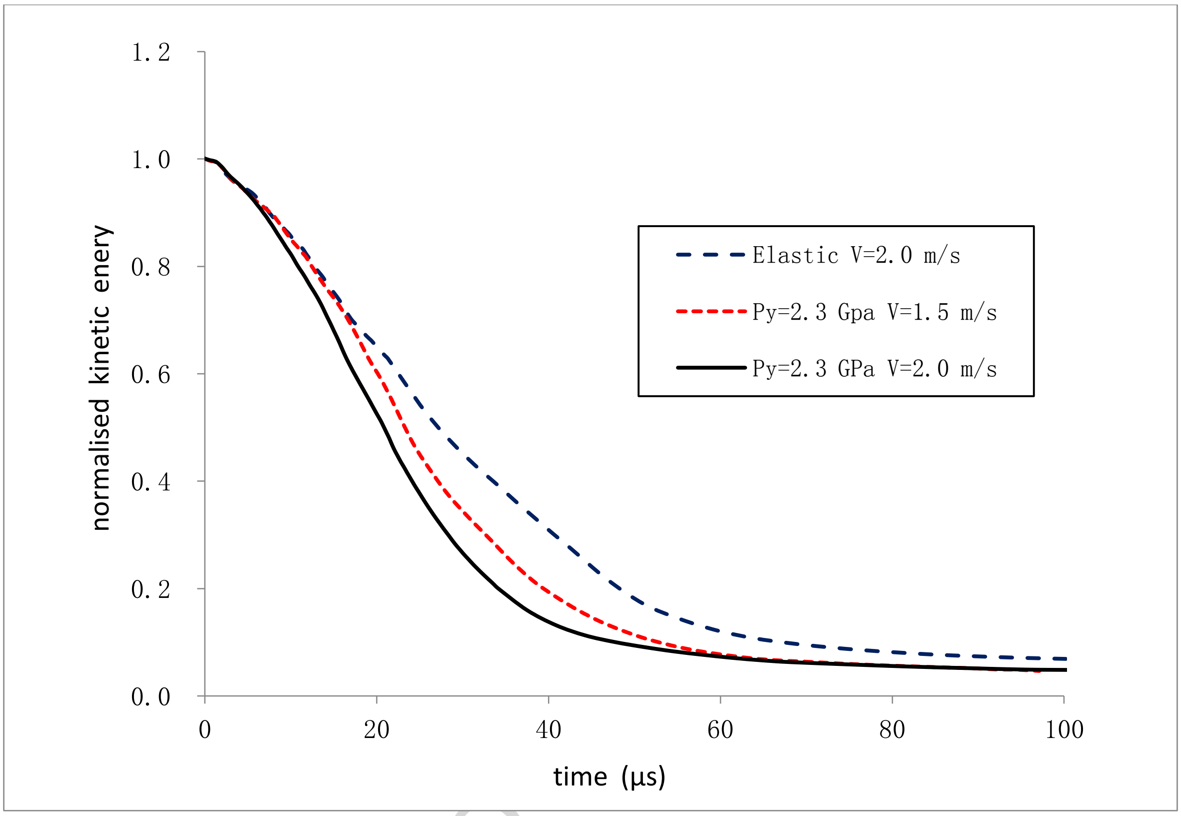

(c) normalised kinetic energy

Fig 7 Influence of velocity on elastic-plastic agglomerate impacts

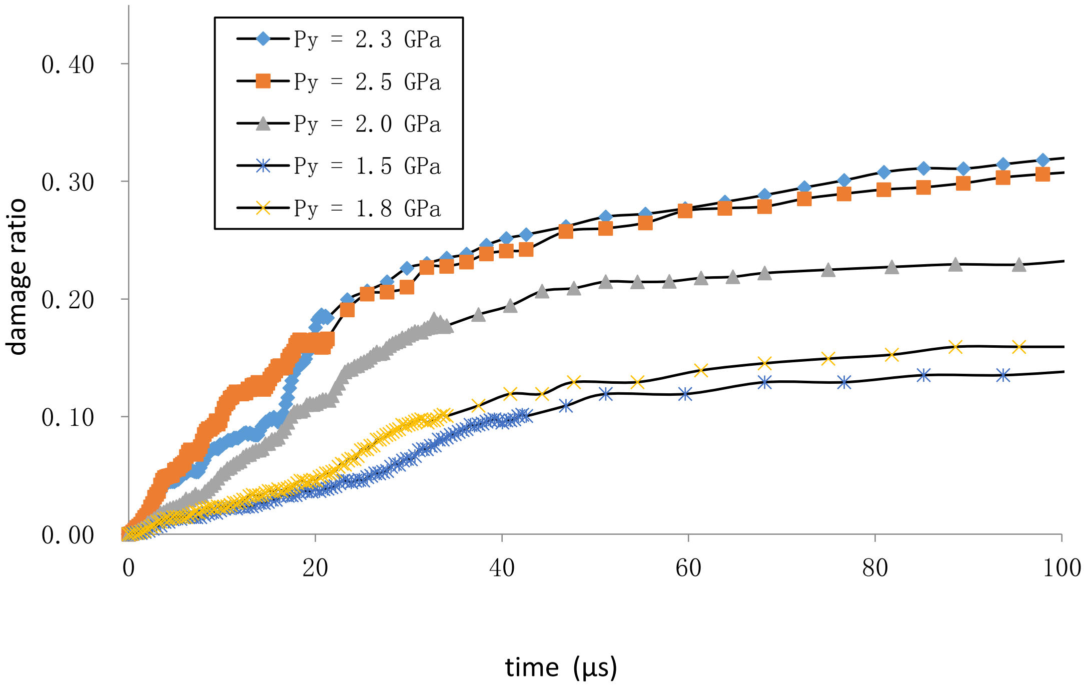

Fig 8 Agglomerate impact damage for different values of the limiting contact pressure p_y (V = 2.0 m/s)

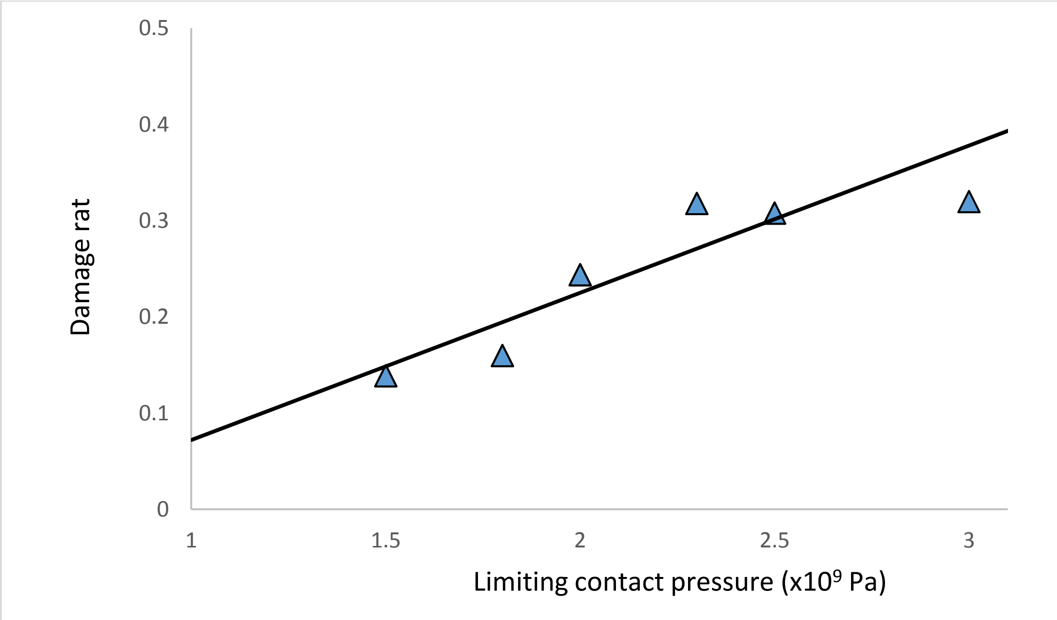

Fig 9 Relationship between limiting contact pressure and damage ratio (V = 2.0 m/s)

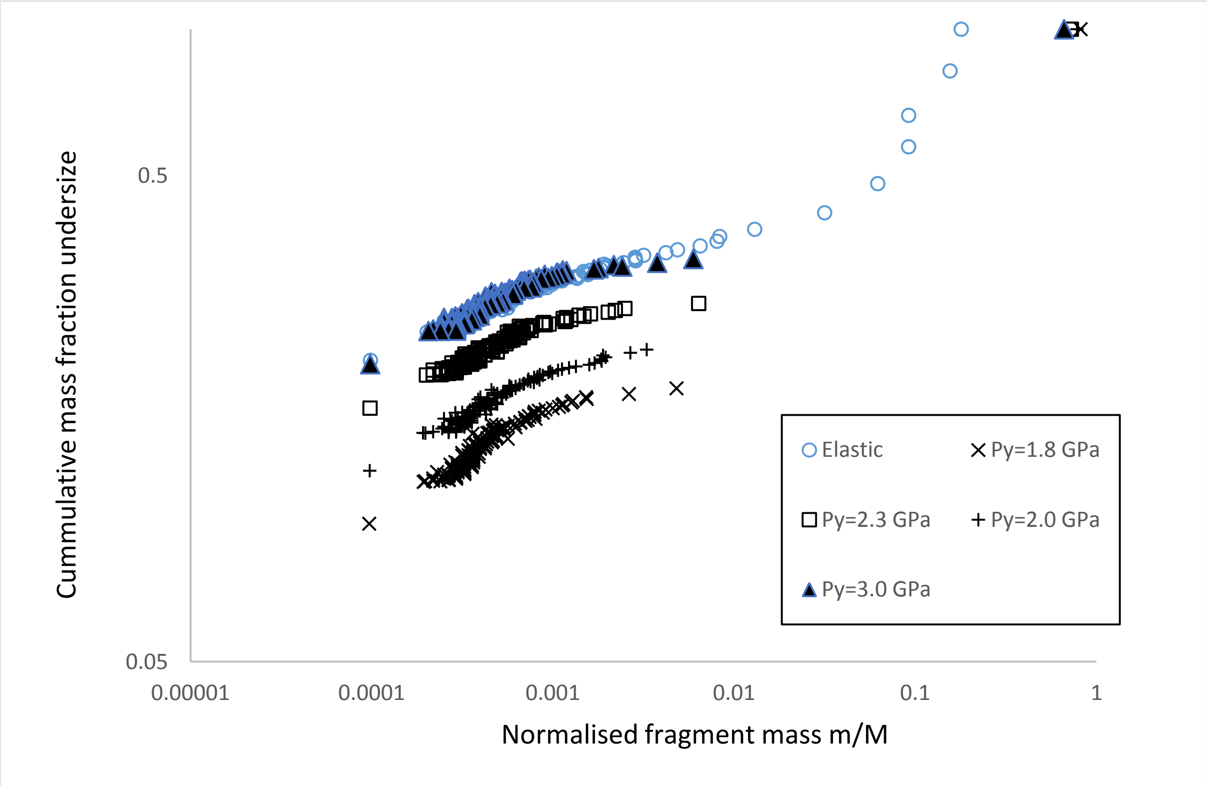

Fig. 10 Fragment size distributions for V = 2 m/s

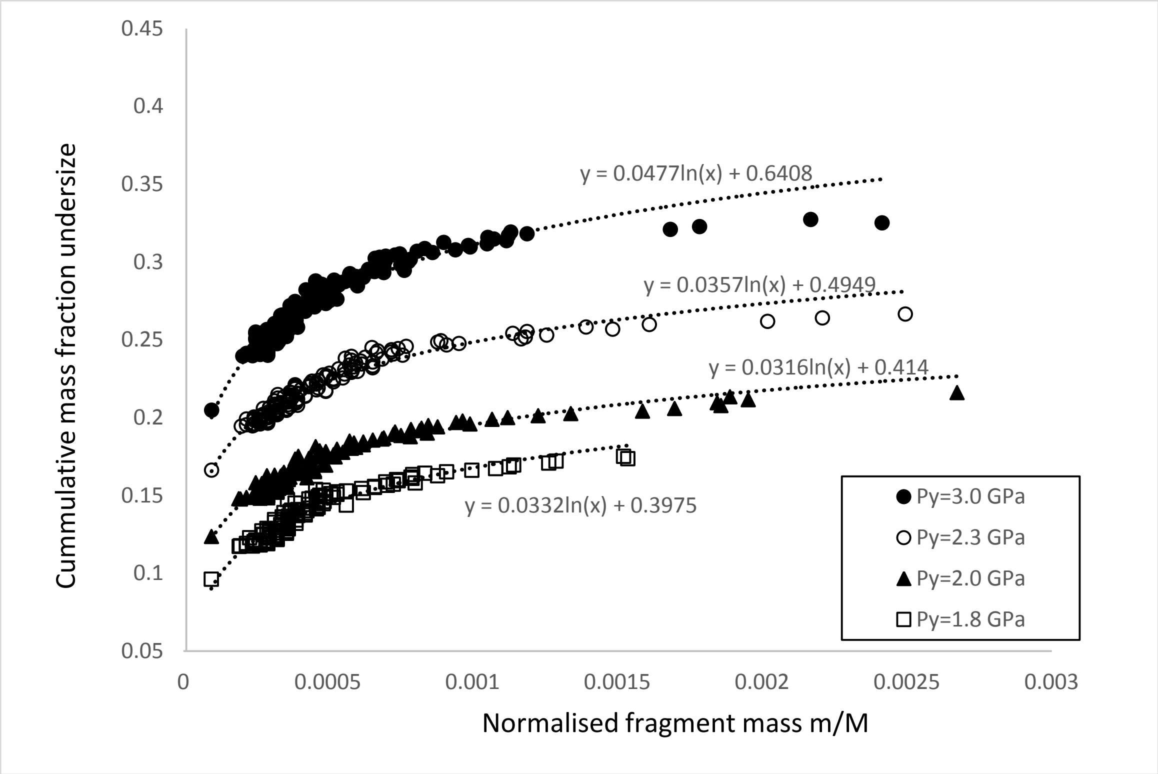

Fig. 11 Trend lines of debris distributions produced from elastic-plastic impacts.

Table 1 Properties of the cuboidal agglomerate

Interface Energy Γ (Jm^{-2})	1.00
Porosity	0.42
Density (kg/m^3)	1153.10
Co-ordination number	3.52

Graphical Abstract

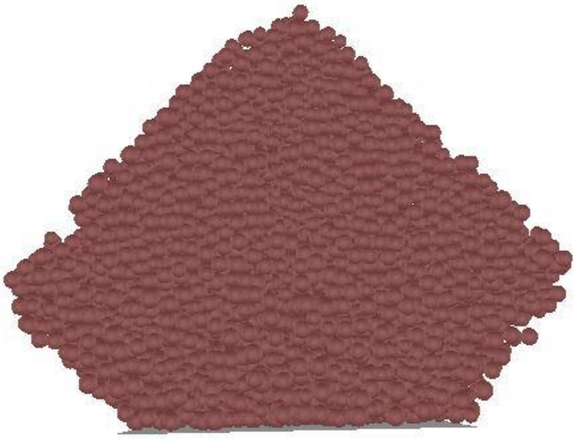

Impact of an agglomerate composed of elastic-plastic particles

Highlights

- Dense agglomerates composed of elastic-plastic primary particles do not fracture.
- Fewer bonds are broken than for the case of elastic particles.
- The particle size distribution of the debris is defined by a logarithmic function.